

COSMOCHEMISTRY

Astronomical context of Solar System formation from molybdenum isotopes in meteorite inclusions

Gregory A. Brennecka^{1,2*}, Christoph Burkhardt², Gerrit Budde^{2,3}, Thomas S. Kruijer^{1,4}, Francis Nimmo⁵, Thorsten Kleine²

Calcium-aluminum-rich inclusions (CAIs) in meteorites are the first solids to have formed in the Solar System, defining the epoch of its birth on an absolute time scale. This provides a link between astronomical observations of star formation and cosmochemical studies of Solar System formation. We show that the distinct molybdenum isotopic compositions of CAIs cover almost the entire compositional range of material that formed in the protoplanetary disk. We propose that CAIs formed while the Sun was in transition from the protostellar to pre-main sequence (T Tauri) phase of star formation, placing Solar System formation within an astronomical context. Our results imply that the bulk of the material that formed the Sun and Solar System accreted within the CAI-forming epoch, which lasted less than 200,000 years.

Calcium-aluminum-rich inclusions (CAIs) are the oldest dated samples of the Solar System and provide a direct record of its formation. These micrometer- to centimeter-sized inclusions in meteorites formed in a high-temperature environment (>1300 K), probably near the young Sun (1), and were subsequently transported outward to the region where carbonaceous chondrite meteorites (and their parent bodies) formed, in which they are found today (2–4). Although some peculiar CAI-like objects, with intrinsic

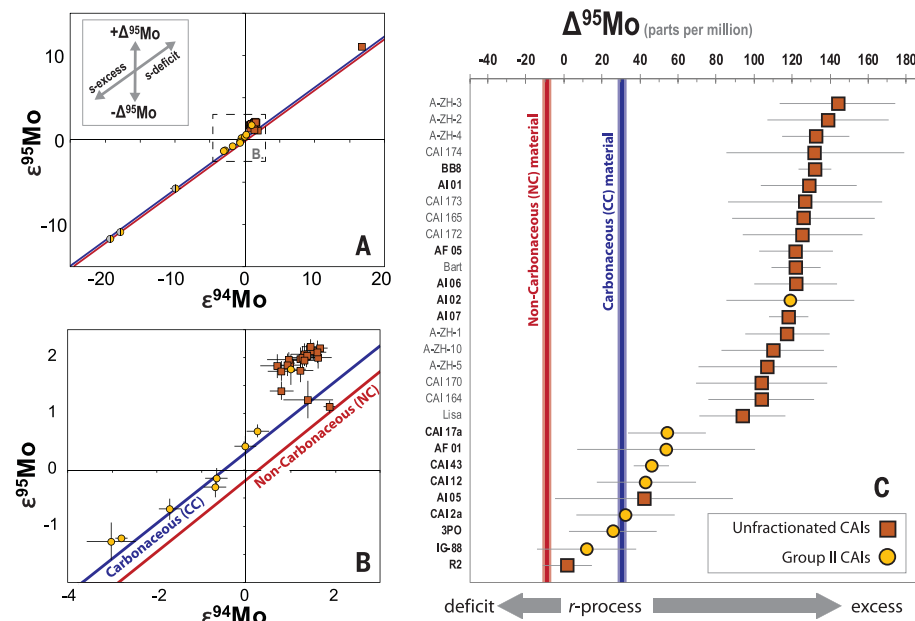
percent-level isotope differences from other Solar System materials, may have formed at a slightly earlier stage [e.g., (5)], the majority of CAIs formed 4567.2 ± 0.2 million years (Myr) ago, over a period of ~40,000 to 200,000 years (6–8). Astronomical observations of young stellar objects (YSOs) show that solar-mass stars accrete by infall from their parental molecular cloud cores before transitioning into pre-main sequence stars surrounded by a disk of gas and dust (referred to as classes 0 to II in the star formation literature) within ~1 Myr (9). This is longer than CAIs took to form, raising the question of which astronomical phase in the Solar System's formation is recorded by the formation of CAIs. Previous work modeling the formation of the Solar System and observations of other stellar systems have associated the formation of CAIs either with the period of collapse and accretion of a protostar (class 0

phase) (1, 6) or with the pre-main sequence, T Tauri phase (class II phase) of the proto-Sun, which would have occurred up to ~1 Myr later (10, 11). Distinguishing between these interpretations would provide a link between astronomical observations of YSOs and the physical samples defining the age of the Solar System.

We investigate this link using the isotopic compositions of CAIs. Previous work has shown that CAIs are isotopically distinct from subsequently formed solids in the solar protoplanetary disk (12, 13), but any “genetic” connections between CAIs and later-formed solids are unclear. Compared with bulk meteoritic materials, CAIs are ¹⁶O-rich and more similar to the Sun than later-formed objects (14). However, because O-isotope variations reflect the complex interplay of mixing and fractionation processes within the protoplanetary disk, and perhaps the parent molecular cloud (14), O isotopes alone are of limited use for linking CAI formation to stellar accretion and disk formation. Another type of isotope variation, known as nucleosynthetic variation, is due solely to inherent isotopic differences in the starting material and can be used to identify temporal and spatial differences in the provenance of Solar System materials. These isotope variations arise from the heterogeneous distribution of presolar material within the disk and show that the protoplanetary disk can be divided into noncarbonaceous (NC) and carbonaceous (CC) reservoirs, which have been suggested to represent the inner and outer Solar System, respectively (15–17). This NC-CC isotopic dichotomy has been demonstrated in several elements, including Mo, which can distinguish between isotope variations arising from the heterogeneous distribution

¹Lawrence Livermore National Laboratory, Livermore, CA, USA. ²Institut für Planetologie, University of Münster, Münster, Germany. ³Division of Geological and Planetary Sciences, California Institute of Technology, Pasadena, CA, USA. ⁴Museum für Naturkunde, Leibniz Institute for Evolution and Biodiversity Science, Berlin, Germany. ⁵Department of Earth & Planetary Sciences, University of California Santa Cruz, Santa Cruz, CA, USA.
*Corresponding author. Email: brennecka2@llnl.gov

Fig. 1. Molybdenum isotopic data for all CAIs in our sample set. (A) $\epsilon^{94}\text{Mo}$ versus $\epsilon^{95}\text{Mo}$ [where ϵ notation represents parts per 10,000 deviation from a terrestrial standard, (20)]. Data plotted are from this work and other studies (12, 18, 25). Samples with half-gray symbols have been excluded from calculations of $\Delta^{95}\text{Mo}$ (20). The CC (blue) and NC (red) correlations (21) are shown for reference. **(B)** Magnified view of the region within the dashed box in (A). **(C)** CAI isotopic variability due to just the r-process, presented using $\Delta^{95}\text{Mo}$ notation (see text for details). The left axis lists the CAIs from literature sources (12, 18, 25) in plain text and those from this study in bold. We have excluded CAIs from the literature that do not have comparable methodologies and CAIs with terrestrial contamination of their Mo isotopic composition. Error bars show 95% confidence intervals. The CC (blue) and NC (red) correlations (21) are shown for reference. In (A) to (C), unfractionated CAIs are plotted with orange squares and group II CAIs with yellow circles.



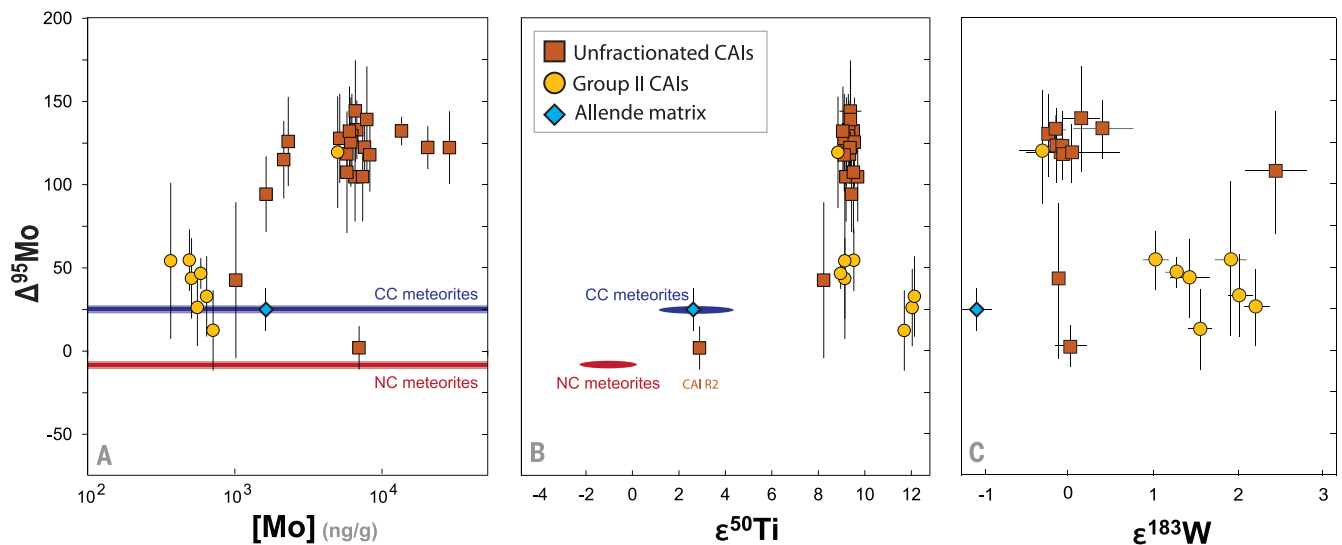


Fig. 2. Isotopic and concentration correlations in CAIs. (A) $\Delta^{95}\text{Mo}$ plotted against concentration of Mo in the CAIs. In general, samples with a lower concentration of Mo also have a lower $\Delta^{95}\text{Mo}$, suggesting at least some disk processing or CAI formation effect on the r-process signature of the CAI. (B) $\Delta^{95}\text{Mo}$ plotted against $\epsilon^{50}\text{Ti}$ in CAIs. See text for discussion of these isotopic signatures in CAIs. (C) $\Delta^{95}\text{Mo}$ plotted against $\epsilon^{183}\text{W}$. The

$\Delta^{95}\text{Mo}$ and $\epsilon^{183}\text{W}$ values do not correlate with one another or show a mixing relationship with the meteorite matrix. This indicates that parent body alteration does not control these signatures. Bulk NC and CC meteorite data for Mo are from (21), Ti data are from (31, 32), and the matrix of the CC meteorite Allende (blue diamonds) is from (16, 28). Other plotting symbols are as in Fig. 1.

of matter produced in the slow (s-process) and rapid (r-process) neutron capture processes of stellar nucleosynthesis (15, 16, 18, 19). Whereas there are large s-process variations among materials within each group, all CC materials are characterized by an approximately constant r-process excess over NC materials. Deviations from pure s-process variation are quantified using the $\Delta^{95}\text{Mo}$ notation [$\Delta^{95}\text{Mo} \equiv (\epsilon^{95}\text{Mo} - 0.596 \times \epsilon^{94}\text{Mo}) \times 100$, where ϵ represents parts per 10,000 deviation from a terrestrial standard (20)], which isolates variation in the amount of r-process Mo from variation in the amount of s-process Mo. Previous studies have shown that the $\Delta^{95}\text{Mo}$ values for the NC reservoir, thought to represent the inner Solar System ($\Delta^{95}\text{Mo} = -9 \pm 2$), and CC reservoir, thought to represent the outer Solar System ($\Delta^{95}\text{Mo} = 26 \pm 2$), are distinct from one another (21). The NC-CC isotopic difference was established within the first ~1 Myr of Solar System history (15), so it likely reflects the incomplete mixing of isotopically variable material infalling from the Sun's protostellar envelope onto the disk at different times (22–24). Molybdenum isotopes, therefore, provide a tool for linking the formation of CAIs to the early processes of infall and disk building and, hence, to a specific stage of star formation.

We measured the Mo isotopic and trace element compositions for a variety of CAIs taken from the carbonaceous chondrite (CV3 group) meteorites Allende (13 CAIs), NWA 6870 (CAI AI01), and NWA 6717 (CAI AI02). We combine these measurements with similar

data from three previous studies (12, 18, 25), which are summarized in table S1. CAIs are classified by their condensation histories, as inferred from their rare earth element (REE) systematics. Hereafter, we refer to samples with unfractionated REE patterns as “unfractionated CAIs,” as distinct from “group II CAIs,” which have fractionated REE patterns, indicating the loss of an ultrarefractory component (26). In addition to Mo, isotopic compositions of the CAIs were determined for several other elements [Ti, Fe, Ni, Sr, Ba, Nd, Sm, Er, Yb, Hf, and W; (20)], all of which are isotopically anomalous in CAIs. The 15 samples newly measured in this study are isotopically consistent with previously published studies of CAIs for these elements and exhibit larger anomalies than bulk meteorites; however, we concentrate on their Mo isotopes (Fig. 1). In general, unfractionated CAIs exhibit less variation in s-process Mo signatures (i.e., $\epsilon^1\text{Mo}$ values; Fig. 1, A and B) and mostly have higher and less variable $\Delta^{95}\text{Mo}$ values (Fig. 1C). By contrast, group II CAIs tend to have more variable s-process Mo signatures (Fig. 1, A and B) and lower $\Delta^{95}\text{Mo}$ values (Fig. 1C). However, a similar overall range in r-process material (>100 parts per million; Fig. 1C) is present in both types regardless of how much s-process variability exists, showing that variations in s-process and r-process Mo nuclides in CAIs are not directly coupled.

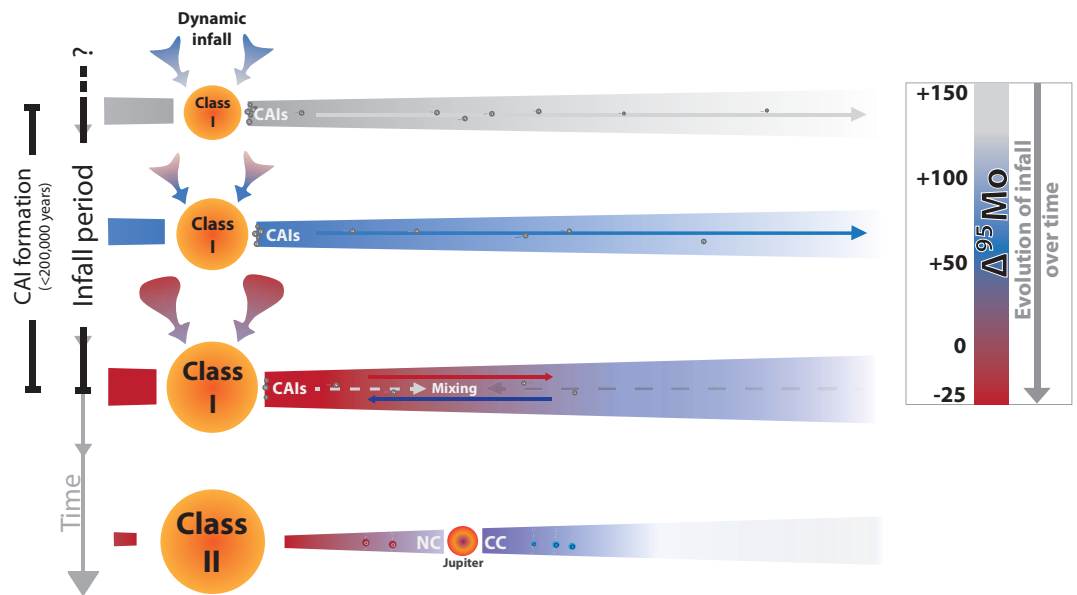
The CAIs exhibit different $\Delta^{95}\text{Mo}$ values, only some of which overlap with the values observed for bulk CC and NC meteorites (Fig.

1C). Unlike the absolute Mo isotope anomalies (i.e., $\epsilon^1\text{Mo}$; Fig. 1, A and B) and the isotope anomalies for other elements (Fig. 2, B and C, and tables S2 and S4), the $\Delta^{95}\text{Mo}$ values provide a link between CAIs and the solid material of the disk as sampled by bulk meteorites. That is, the composition of CAIs varies from larger r-process excesses (more positive $\Delta^{95}\text{Mo}$) toward more NC-like compositions.

We interpret the distinct $\Delta^{95}\text{Mo}$ values for these CAIs by relating them to models of how the $\Delta^{95}\text{Mo}$ values of the NC and CC reservoirs may have been established. These models demonstrate that during infall of the Solar System's parental molecular cloud, the isotopic composition of the infalling material changed from high $\Delta^{95}\text{Mo}$ values in the early stages to lower, NC-like $\Delta^{95}\text{Mo}$ values toward the final stage; and that as a result of viscous spreading of the initial disk, the bulk of the mass of the inner protoplanetary disk comes from the later infall, whereas the outer disk contains a higher proportion of early infalling material (4, 22–24). The rapid outward transport of material during the initial disk-building process provides a mechanism for the transport of CAIs from near the Sun to the outer Solar System (2–4). Within this framework, the range of $\Delta^{95}\text{Mo}$ in CAIs extending from values characteristic of early infall (higher than the CC reservoir) to that of bulk meteorites may have three potential origins: (i) exchange of Mo with the host meteorite during alteration on the parent body; (ii) changes in the isotopic composition of infall, and, hence,

Fig. 3. Schematic diagram of the early evolution of the Solar System.

The diagram is modeled after (22) but modified to reflect our interpretation of the CAI data and associated stages of stellar evolution. Heterogeneous infall from the Sun's parent molecular cloud evolves from a higher to lower amount of r-process material (i.e., higher to lower $\Delta^{95}\text{Mo}$, indicated by the color bar). The isotopic compositions of CAIs record this change in composition and subsequent processing within the disk. The formation of CAIs occurs during the transition of the Sun from a class I to class II YSO in less than 200,000 years.



the gas from which CAIs condensed; or (iii) processing of CAIs within the disk before incorporation into their host meteorite.

Group II CAIs have substantially lower concentrations of Mo than unfractionated CAIs and so are more susceptible to alteration in their Mo isotopic composition than unfractionated CAIs. This may explain why group II samples tend to have lower (more bulk meteorite-like) $\Delta^{95}\text{Mo}$ values, although two unfractionated CAIs (AI05 and R2) also show such isotopic compositions. Nevertheless, because the $\Delta^{95}\text{Mo}$ values of many group II CAIs are similar to those of the matrix in Allende (16), their $\Delta^{95}\text{Mo}$ values may potentially reflect exchange with the host meteorite on the parent body. However, W, which is thought to behave similarly to Mo during parent-body alteration (27), is also strongly depleted in group II CAIs, yet all group II CAIs with low $\Delta^{95}\text{Mo}$ exhibit positive $\epsilon^{183}\text{W}$ signatures, unlike the negative $\epsilon^{183}\text{W}$ of the matrix of CV3 chondrites (28). This indicates that parent-body alteration is not the source of the signatures. As such, the combined Mo-W isotopic signatures of group II CAIs are difficult to account for solely by parent-body processes. This is also true for the large range of $\epsilon^1\text{Mo}$ values in group II CAIs (Fig. 1, A and B) and for the isotopic variation in unfractionated CAIs. Thus, although parent-body processes may have modified Mo isotope signatures in some group II CAIs, they cannot account for most of the isotopic variations that we see (see supplementary text). Consequently, the range of $\Delta^{95}\text{Mo}$ in CAIs was likely acquired before chondrite parent body accretion, either during CAI condensation or subsequent processing of CAIs within the disk.

If the range of $\Delta^{95}\text{Mo}$ in CAIs directly recorded the change of the isotopic composition of infall and, hence, of the gas from which

CAIs condensed, CAIs should also directly record changes in other isotope systems that distinguish between NC and CC compositions, such as Ti. Bulk NC meteorites are characterized by negative $\epsilon^{50}\text{Ti}$ anomalies down to about -2 , whereas the majority of CAIs have $\epsilon^{50}\text{Ti}$ excesses around $+9$ [e.g., (29)]. Thus, if evolving infall from the molecular cloud was the sole cause of isotopic anomalies in CAIs, then $\Delta^{95}\text{Mo}$ should coevolve with $\epsilon^{50}\text{Ti}$ in CAIs, assuming that Mo and Ti had similar carriers. However, with one exception—CAI R2, which exhibits both low $\Delta^{95}\text{Mo}$ and low $\epsilon^{50}\text{Ti}$ —no such clear coevolution is observed (Fig. 2B). A change of infalling matter toward NC-like compositions, which is characterized by $\epsilon^{183}\text{W} \sim 0$, also does not provide a viable explanation for the positive $\epsilon^{183}\text{W}$ values of group II CAIs. Together, these observations suggest that dynamic infall from the molecular cloud (Fig. 3) cannot be the sole cause of the observed isotopic signatures in CAIs. We propose that even though dynamic infall initially generated the range of $\Delta^{95}\text{Mo}$ variations within the disk, additional processing within the protoplanetary disk established the measured isotopic signatures of CAIs. This processing evidently did not affect $\epsilon^{50}\text{Ti}$, which shows little variation among the CAIs we studied but resulted in substantial and uncorrelated anomalies of $\epsilon^1\text{Mo}$ and $\epsilon^{183}\text{W}$. The reasons for this disparate behavior during processing are unclear, but they may include different thermal properties of the carriers involved, size or density sorting of these carriers, and chemical fractionations during CAI formation, which made Mo and W more susceptible to isotopic modifications by processes within the disk.

The range of $\Delta^{95}\text{Mo}$ values in CAIs covers almost the entire compositional range ob-

served among bulk meteorites, suggesting that CAIs acquired their isotopic signatures when the Sun's protoplanetary disk had largely formed. This links CAI formation to a class II protostar, which is consistent with evidence of the short-lived isotope ^{10}Be in CAIs (11) and noble gas signatures from hibonite inclusions (30)—refractory inclusions thought to have formed before the more common CAIs—indicating that these refractory objects formed when the Sun was a T Tauri star.

Because the vast majority of CAIs are thought to have formed within $\sim 40,000$ to $200,000$ years (6–8), the recorded isotopic character of CAIs also represents an amount of time in which that isotopic character was established. Interpreting the isotopic compositions of CAIs in the framework of disk evolution models, and with the knowledge that CAIs formed close to the young Sun in a known time window, we constrain the primary accretion phase (i.e., classes I and II) of stars like the Sun to less than 200,000 years, consistent with astronomical observations of YSOs (9).

REFERENCES AND NOTES

1. J. A. Wood, *Geochim. Cosmochim. Acta* **68**, 4007–4021 (2004).
2. E. Jacquet, S. Fromang, M. Gounelle, *Astron. Astrophys.* **526**, L8 (2011).
3. F. C. Pignatelle, S. Charnoz, M. Chaussidon, E. Jacquet, *Astrophys. J. Lett.* **867**, 23 (2018).
4. L. Yang, F. J. Ciesla, *Met. Planet. Sci.* **47**, 99–119 (2012).
5. L. Kööp et al., *Geochim. Cosmochim. Acta* **189**, 70–95 (2016).
6. J. N. Connelly et al., *Science* **338**, 651–655 (2012).
7. N. Kawasaki et al., *Earth Planet. Sci. Lett.* **511**, 25–35 (2019).
8. G. J. MacPherson, N. T. Kita, T. Ushikubo, E. S. Bullock, A. M. Davis, *Earth Planet. Sci. Lett.* **331–332**, 43–54 (2012).
9. L. Cieza et al., *Astrophys. J.* **667**, 308–328 (2007).
10. F. J. Ciesla, *Icarus* **208**, 455–467 (2010).
11. N. Dauphas, M. Chaussidon, *Annu. Rev. Earth Planet. Sci.* **39**, 351–386 (2011).
12. G. A. Brennecka, L. E. Borg, M. Wadhwa, *Proc. Natl. Acad. Sci. U.S.A.* **110**, 17241–17246 (2013).

13. N. Dauphas, E. A. Schauble, *Annu. Rev. Earth Planet. Sci.* **44**, 709–783 (2016).
14. K. D. McKeegan *et al.*, *Science* **332**, 1528–1532 (2011).
15. T. S. Kruijjer, C. Burkhardt, G. Budde, T. Kleine, *Proc. Natl. Acad. Sci. U.S.A.* **114**, 6712–6716 (2017).
16. G. Budde *et al.*, *Earth Planet. Sci. Lett.* **454**, 293–303 (2016).
17. P. H. Warren, *Earth Planet. Sci. Lett.* **311**, 93–100 (2011).
18. C. Burkhardt *et al.*, *Earth Planet. Sci. Lett.* **312**, 390–400 (2011).
19. G. M. Poole, M. Rehkämper, B. J. Coles, T. Goldberg, C. L. Smith, *Earth Planet. Sci. Lett.* **473**, 215–226 (2017).
20. Materials and methods are available as supplementary materials.
21. G. Budde, C. Burkhardt, T. Kleine, *Nat. Astron.* **3**, 736–741 (2019).
22. J. A. M. Nanne, F. Nimmo, J. N. Cuzzi, T. Kleine, *Earth Planet. Sci. Lett.* **511**, 44–54 (2019).
23. C. Burkhardt, N. Dauphas, U. Hans, B. Bourdon, T. Kleine, *Geochim. Cosmochim. Acta* **261**, 145–170 (2019).
24. E. Jacquet, F. C. Pignatole, M. Chaussidon, S. Charnoz, *Astrophys. J.* **884**, 32 (2019).
25. Q. R. Shollenberger *et al.*, *Geochim. Cosmochim. Acta* **228**, 62–80 (2018).
26. A. M. Davis, L. Grossman, *Geochim. Cosmochim. Acta* **43**, 1611–1632 (1979).
27. P. J. Sylvester, B. J. Ward, L. Grossman, I. D. Hutcheon, *Geochim. Cosmochim. Acta* **54**, 3491–3508 (1990).
28. G. Budde, T. Kleine, T. S. Kruijjer, C. Burkhardt, K. Metzler, *Proc. Natl. Acad. Sci. U.S.A.* **113**, 2886–2891 (2016).
29. A. M. Davis *et al.*, *Geochim. Cosmochim. Acta* **221**, 275–295 (2018).
30. L. Kööp *et al.*, *Nat. Astron.* **2**, 709–713 (2018).
31. A. Trinquier *et al.*, *Science* **324**, 374–376 (2009).
32. J. Zhang, N. Dauphas, A. M. Davis, I. Leya, A. Fedkin, *Nat. Geosci.* **5**, 251–255 (2012).

ACKNOWLEDGMENTS

We thank A. Bischoff for helpful discussions and J. Render and Q. Shollenberger for support and helpful comments on an early draft of this manuscript. We thank N. Marks and B. Jacobsen for assistance with the petrography. We acknowledge the efforts of U. Heitmann for the initial preparation of many of these samples. Allende CAI samples CAI 43 and BB8 were obtained from the collection of the American Museum of Natural History (AMNH) (New York, USA). D. S. Ebel and S. Wallace (Earth and Planetary Sciences, AMNH); R. Matthes, L. Schultz, and L. L. Pryer (Siemens Medical Solutions, Cary, NC); R. Smith (NC Museum of Natural Sciences); and J. Thorstenson (Duke University) are thanked for their support and for providing access to computerized tomography scanners. **Funding:** G.A.B. was supported by a Sofja Kovalevskaja award from the Alexander von Humboldt Foundation. The Deutsche Forschungsgemeinschaft as part of the Research Priority Program SPP 1385 supported T.S.K. (grant KR 4463/1) and T.K. (grant KL 1857/4). An Annette Kade Fellowship (to G.B.) supported characterization of two CAI samples. This study

was performed under the auspices of the U.S. Department of Energy by Lawrence Livermore National Laboratory under contract DE-AC52-07NA27344 with release number LLNL-JRNL-802017. **Author contributions:** G.A.B., C.B., and G.B. analyzed samples; G.A.B., C.B., T.S.K., and T.K. devised the project; and all authors contributed to interpretation of the data and writing the manuscript. **Competing interests:** The authors declare no competing interests. **Data and materials availability:** All data are available in tables S1 to S6. Newly measured CAIs were taken from fragments of the meteorites Allende, NWA 6870, and NWA 6717, all of which are curated at the Institut für Planetologie, University of Münster, Germany, except samples CAI 43 and BB8, which were obtained from a fragment of Allende curated at the AMNH, New York, USA. The CAI samples were consumed during the experiments.

SUPPLEMENTARY MATERIALS

science.sciencemag.org/content/370/6518/837/suppl/DC1
Materials and Methods
Supplementary Text
Figs. S1 to S7
Tables S1 to S6
References (33–63)

14 October 2019; accepted 16 September 2020
10.1126/science.aaz8482

Astronomical context of Solar System formation from molybdenum isotopes in meteorite inclusions

Gregory A. Brennecka, Christoph Burkhardt, Gerrit Budde, Thomas S. Kruijer, Francis Nimmo and Thorsten Kleine

Science **370** (6518), 837-840.
DOI: 10.1126/science.aaz8482

Timing Solar System formation

The oldest solids that formed in the Solar System are calcium-aluminium-rich inclusions (CAIs), small metallic droplets that were later incorporated into meteorites. The ages of CAIs are conventionally taken as the age of the Solar System, but which exact moment in star formation they correspond to has been unclear. Brennecka *et al.* measured molybdenum isotope ratios in CAIs and found a wide range of origins in both the inner and outer Solar System. They propose that CAIs formed from heterogeneous material accreting from the presolar nebula and that the ages of CAIs coincide with the Sun's transition from a protostar to a pre-main sequence star.

Science, this issue p. 837

ARTICLE TOOLS

<http://science.sciencemag.org/content/370/6518/837>

SUPPLEMENTARY MATERIALS

<http://science.sciencemag.org/content/suppl/2020/11/11/370.6518.837.DC1>

REFERENCES

This article cites 63 articles, 8 of which you can access for free
<http://science.sciencemag.org/content/370/6518/837#BIBL>

PERMISSIONS

<http://www.sciencemag.org/help/reprints-and-permissions>

Use of this article is subject to the [Terms of Service](#)

Science (print ISSN 0036-8075; online ISSN 1095-9203) is published by the American Association for the Advancement of Science, 1200 New York Avenue NW, Washington, DC 20005. The title *Science* is a registered trademark of AAAS.

Copyright © 2020 The Authors, some rights reserved; exclusive licensee American Association for the Advancement of Science. No claim to original U.S. Government Works